# EFFECT OF INERTIAL TAIL ON YAW RATE OF 45 GRAM LEGGED ROBOT*

N.J. KOHUT, D. W. HALDANE
*Department of Mechanical Engineering, University of California, Berkeley*
*Berkeley, CA 94709, USA*

D. ZARROUK, R.S. FEARING
*Department of Electrical Engineering, University of California, Berkeley*
*Berkeley, CA 94709, USA*

## 1. Introduction

Small legged robots have unique potential for widespread application in search and rescue, hazardous exploration, battlefield reconnaissance, and almost any remote, inaccessible or dangerous situation not reachable by humans. Dynamic running robots have used a variety of steering means, including differential velocity drive [1][2] and actively changing leg kinematics [3][4]. Previous robots have also used tails for various functions, such as turning in an aquatic environment [5], active pitch control [6][7], or stabilization during climbing [8]. The robot discussed here uses a tail to produce a turn on rough or flat ground. This paper examines the way in which this is done, through the use of angular momentum exchange and internal impacts that generate a turning impulse.

## 2. Description of Robot and Model

### 2.1 *The TAYLRoACH Robot*

The TAYLRoACH (Tail Actuated Yaw Locomotion RoACH) is a 45 gram robot that features three 7 mm brushed DC motors, two which independently control a set of 3 legs on one side of the robot. It is an evolution of the OctoRoACH platform [2], with a similar configuration. TAYLRoACH is also equipped with a 4 gram, 11.5 cm tail, driven by a custom gearbox and the third DC motor. This gives the tail a moment of inertia of $5.3 \times 10^{-5}$ kg-m$^2$ about its

* This work was supported by the Army Research Laboratory under the Micro Autonomous Systema and Technology Collaborative Technology Alliance.

base, while the TAYLRoACH has a moment of inertia of $2.3x10^{-4}$ kg-m$^2$ about its center of mass. The center of mass of the body is located 6 cm away from the base of the tail.

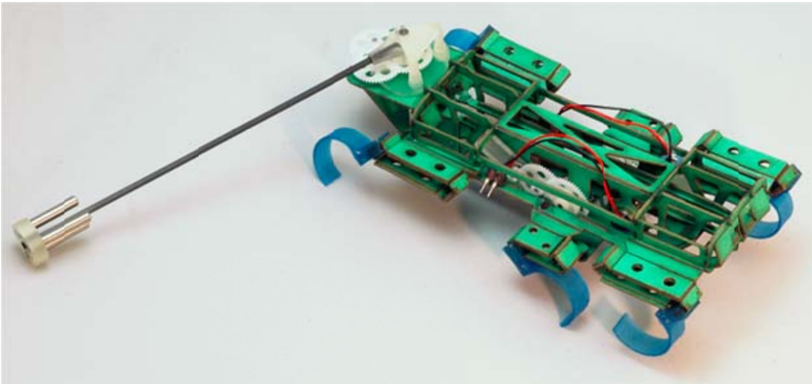

Figure 1: The TAYLRoACH robot. Electronics and battery have been removed to show the body.

The gearbox for the tail features an 85.3:1 ratio for high acceleration. It is also equipped with two stops that limit the rotation of the tail to approximately $260^0$ statically. These stops may decelerate the tail quickly, producing forces from impact.

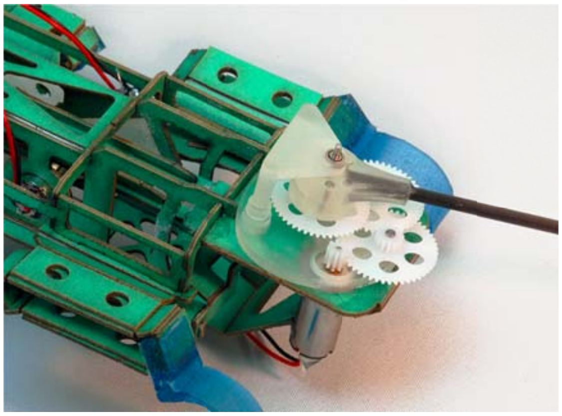

Figure 2: The tail gearbox, with stops.

**2.2 *Model***

Below, we see an abstract representation of the tail-body system.

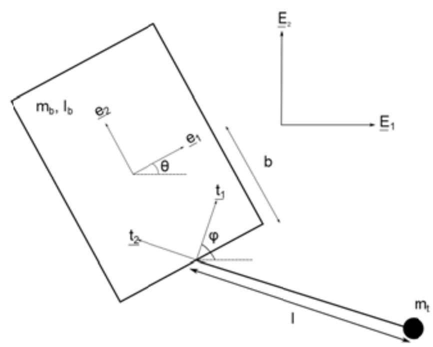


Figure 3: A 2D model for the tail and body.

The body has mass $m_b$ and inertia $I_b$ about the body's center of mass, while the tail consists of a massless rod and a point mass $m_t$. The body's angle with respect to the world frame is $\theta$, and the tail's angle with respect to the world frame is φ. The distance from the body's center of mass to the center of the tail's rotation is $b$. From here, we can express the angular momentum about the center of mass of the body-tail system as

$$\boldsymbol{H}_{COM} = \boldsymbol{I_b}\boldsymbol{\omega_b} + \boldsymbol{r}_{b,COM} \times m_b \boldsymbol{v}_{b,COM} + \boldsymbol{r}_t \times m_{\boldsymbol{t}} \boldsymbol{v}_{t,COM}$$

If no friction or other external torques were present, angular momentum would be conserved, and the rotation of the body would be a function of the rotation of the tail and the total angular momentum [6]. However, friction is present and changes things significantly. If the tail moves slowly, no motion of the body may occur at all, due to friction holding the body in place. If the tail moves quickly, the friction can be overcome, turning the body. Additionally, if the tail hits the hard stop at the end of its travel, a moment may be produced by the impact to turn the robot. This turn will be opposite in direction to the turn caused by tail movement. The friction is a result of six moving, flexible legs with varying contact. A detailed discussion of the friction will not be undertaken here, but it warrants further study.

## 3. Experiment and Results

TAYLRoACH was driven from a stop on a tile surface at a fixed throttle for the legs for two seconds. The tail is initially set to its full right position, and is free, with no torque applied to it. Velocity control is implemented on the leg speeds, but neither position control of the legs nor steering control of the body is used. This means that the phasing of the left and right legs is not controlled, and there is no feedback on the robot heading to ensure straight ahead motion. One second into the experiment, the tail is actuated with maximum torque for 300 milliseconds moving the tail from full right to full left position. Yaw data for the tail and body were recorded using an OptiTrack [9] motion capture system.

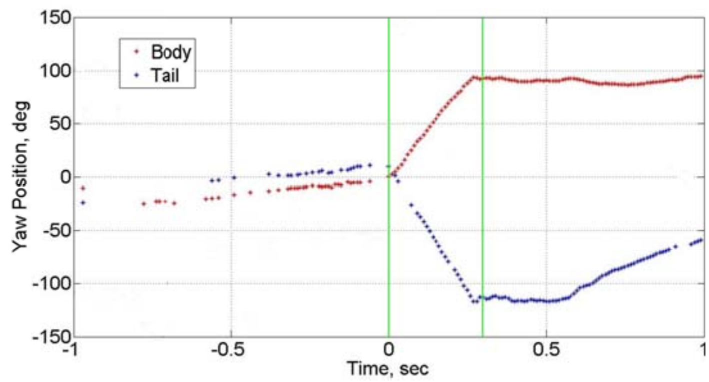


Figure 4: Data from an example trial showing the yaw displacement of the body and tail with respect to time. At the beginning of the trial the robot moves forward without any steering input. At the first vertical line, the tail is actuated. This actuation ends at the second vertical line while the robot continues running.

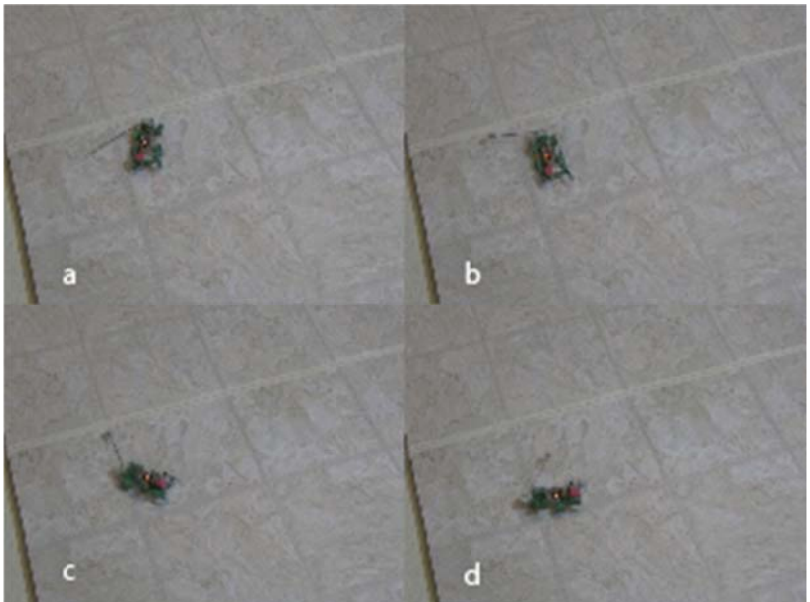

Figure 5: Stills from a video showing the robot turn approximately $90^0$. a) t = 0s, b) t = 0.10s, c) t = 0.23s, d) t = 0.37s

As seen in figure 4, the robot drifts before tail actuation, has a high yaw rate during the tail actuation, and then changes direction after the tail actuation, possibly due to an internal impact. TAYLRoACH is a small, minimally actuated robot, and many variables, such as ground contact, roll, pitch, and leg position are not controlled during this experiment. This leads to variation among trials, shown in figure 5.

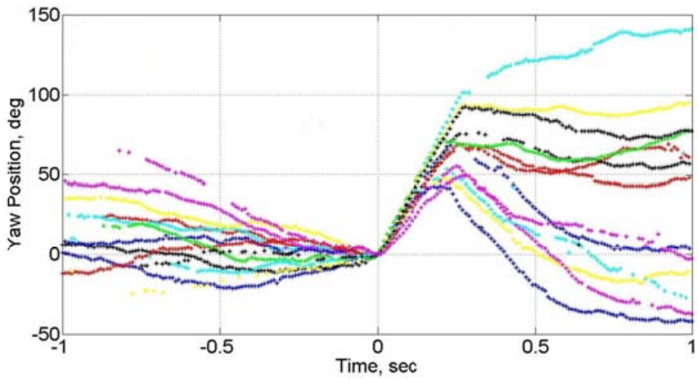


Figure 6: Body yaw vs. time. Fourteen trials were used to measure the variation in behavior. This plot is normalized so that at the point of tail actuation, time and body yaw are zero.

We break these data into three events: before tail actuation, during tail actuation, and after tail actuation. We find that each event has distinct characteristics.

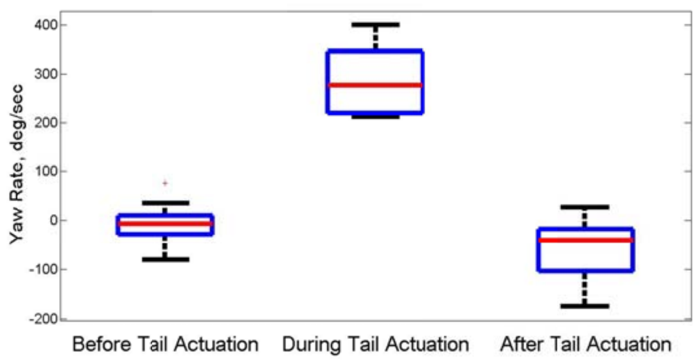


Figure 7: Body yaw rate, before, during, and after tail actuation. Red line marks mean, blue box marks one standard deviation, and black bars mark minimum and maximum values.

As shown in figure 7, yaw rate is very high during tail actuation (mean $348^0$ $sec^{-1}$). Before tail actuation, mean yaw rate is basically zero ($-7^0$ $sec^{-1}$), suggesting the robot is going on average straight, though it is still subject to variation. After tail actuation, average yaw rate is $-41^0$ $sec^{-1}$. The difference in yaw rate before and after actuation (both periods in which the tail is unactuated and free) may be accounted for by the impact of the tail. This impact reduces the total turn angle of the robot and is undesired. Since these yaw rates are measured over different time periods, it is useful to look at the total yaw as well.

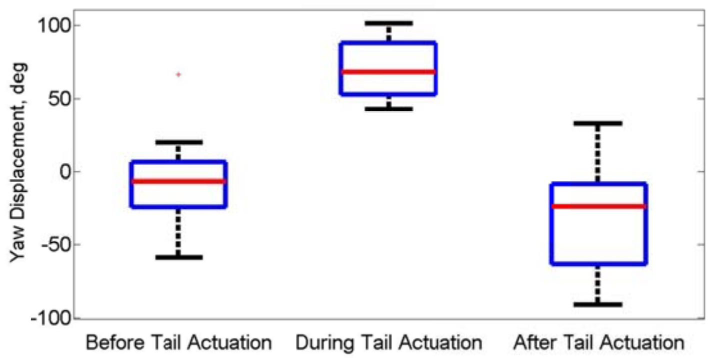


Figure 8: Mean, standard deviation, min, and max of yaw displacement, before, during, and after tail actuation.

In figure 8 we see that the yaw displacement before actuation is small ($7^0$), while it is large during actuation ($68^0$) and after actuation ($-24^0$). The impact of the tail decreases the total turn of the robot, on average, by 35%.

## 4. Discussion and Conclusion

Using a tail to turn a legged robot running over ground is a complex phenomenon. Several factors, such as leg contact, normal load, surface variation, and others, can determine the amount of friction and constraint forces imposed on a robot during a turn. Additionally, the dynamics and mechanical constraints of the tail show high performance during tail actuation, but this can be mitigated by impact forces which reduce the overall turn angle and increase the settling time of the robot.

Overall performance can be very high, producing net turns of $90^0$ at $300^0$ $sec^{-1}$. However, the variation shown needs to be accounted for and controlled for consistent high performance. Controlling leg position may be crucial to this, as currently the left and right sides of the robot are driven independently without phase locking. In addition, developing a running gait with a predictable airborne phase may allow a tail actuation during a period where no friction is present, giving more repeatable results. Finally, position sensing on the tail will allow more intelligent control.

**Acknowledgments**

We would like to thank the Army Research Laboratory and the Micro Autonomous Systems and Technology Collaborative Technology Alliance for supporting this work. We would also like to thank Kevin Peterson, Fernando Garcia Bermudez, and Andrew Pullin for help with figure preparation, OptiTrack operation, and Python support, respectively.

**References**

1. U. Saranli, M. Buehler, and D.E. Koditschek, "RHex: A simple and highly mobile hexapod robot," *The Int. J. of Robotics Research*, vol. 20, no. 7, pp. 616-631, 2001.
2. A.O. Pullin, N.J. Kohut, D. Zarrouk, R.S. Fearing, "Dynamic turning of 13 cm robot comparing tail and differential drive," to appear in *IEEE International Conference on Robotics and Automation*, May 2012.
3. J.G. Cham, S.A. Bailey, J.E. Clark, R.J. Full, and M.R. Cutkosky, "Fast and Robust: Hexapedal robots via shape deposition and manufacturing," *The Int. J. of Robotics Research,* vol. 21, no. 10-11, pp. 869-882, 2002.
4. A. McClung, "Techniques for dynamic maneuvering of hexapedal legged robots," Ph. D. dissertation, Stanford University, 2006.
5. K. Hirata, T. Takimoto, K. Tamura, "Study on turning performance of a fish robot," in *First International Symposium on Aqua Bio-Mechhanisms*, August 2000.
6. T. Libby, T. Y. Moore, E. Chang-Siu, D. Li, D. J. Cohen, A. Jusufi, R. J. Full, "Tail-assisted pitch control in lizards, robots, and dinosaurs." *Nature*, vol. 481, pp. 181-184, 2012.
7. E. Chang-Siu, T. Libby, M Tomizuka, R. Full, "A Lizard-Inspired Active Tail Enables Rapid Maneuvers and Dynamic Stabilization in a Terrestrial Robot," IEEE International Conference on Intelligent Robots and Systems, September 2011.
8. W. Provancher, S. Jensen-Segal, M. Fehlberg, "ROCR: An Energy-Efficient Dynamic Wall Climbing Robot," *IEEE Transactions on Mechatronics,* October 2011, vol. 16 no. 5, pp. 897-906.
9. http://www.naturalpoint.com/optitrack/